**Advancing Electrocatalytic Nitrogen Fixation: Insights from Molecular Systems**

| | |
|---|---|
| Journal: | *Faraday Discussions* |
| Manuscript ID | FD-ART-01-2023-000017.R1 |
| Article Type: | Paper |
| Date Submitted by the Author: | 03-Feb-2023 |
| Complete List of Authors: | Peters, Jonas; California Institute of Technology, Chemistry and Chemical Engineering |
| | |

SCHOLARONE™
Manuscripts

# ADVANCING ELECTROCATALYTIC NITROGEN FIXATION: INSIGHTS FROM MOLECULAR SYSTEMS

**Jonas C. Peters**

**California Institute of Technology**

**Pasadena CA 91125**

## ABSTRACT

Nitrogen fixation has a rich history within the inorganic chemistry community. In recent years attention has (re)focused on developing electrocatalytic systems capable of mediating the nitrogen reduction reaction ($N_2RR$). Well-defined molecular catalyst systems have much to offer in this context. This personal perspective summarizes recent progress from our laboratory at Caltech, pulling together lessons learned from a number of studies we have conducted, placing them within the broader context of thermodynamic efficiency and selectivity for the $N_2RR$. In particular, proton-coupled electron transfer (PCET) provides an attractive strategy to achieve enhanced efficiency for the multi-electron/proton reduction of $N_2$ to produce $NH_3$ (or $NH_4^+$), and electrocatalytic PCET (*e*PCET) via an *e*PCET mediator affords a promising means of mitigating HER such that the $N_2RR$ can be achieved in a catalytic fashion.

## INTRODUCTION.

The benefits of ammonia ($NH_3$) as a fertilizer source in agriculture have been recognized for over 150 years. The industrial synthesis of $NH_3$, with its origins tied closely to Axis Powers saltpeter supply chain challenges during WWI, became one of the most transformative technologies of the 20th century. It now helps sustain the food supply for billions of people worldwide.[1] Chemists have long wondered if an electrical alternative to the Haber-Bosch process is technologically feasible. The idea of using electricity to drive the nitrogen ($N_2$) reduction reaction ($N_2$RR) to produce ammonia finds an early proof-of-concept from Mother Nature, where high-energy lightning plasma combines $N_2$ and water to produce $NH_3$ (and also nitrates), contributing modestly to natural sources of fixed $NH_3$. Scientists have used low-voltage arc lamps and high-energy laboratory plasmas to attempt to replicate this process in the laboratory and industry.[2,3,4]

Such high-energy approaches to nitrogen fixation fall short in terms of the efficiency (and selectivity) needed for practical applications. To address this, and to be able to exploit $NH_3$ as an energy vector in addition to its use in fertilizer, researchers are looking for ways to use electricity, specifically electrocatalysis, to combine $N_2$ with H-atom equivalents in more efficient and selective ways. Indeed, electrochemistry already has an early foothold. Performing water electrolysis to derive $H_2$ (instead of steam reforming of methane) and then coupling the $H_2$ with $N_2$ via Haber-Bosch to produce $NH_3$ is achievable and is already being explored for technoeconomic feasibility in industrial settings.[5,6] But electrocatalysis can offer more direct means of reducing $N_2$ without the need to generate $H_2$ as an intermediate. Such an approach may have practical advantages related to cost, net energy efficiency, and more distributed production close to end use.[7,8,9]

The majority of direct electrocatalytic $N_2$R (nitrogen reduction) research efforts come from the heterogeneous catalysis community.[10] Reports in this field are appearing at an increasingly rapid clip, readily captured graphically via an unconstrained topic search of the Web of Science, using the descriptor "electrocatalytic ammonia synthesis" (Figure 1). A healthy degree of caution is warranted in considering the experimental results reported in this growing body of literature. As continues to be underscored, analysis of and accounting for $NH_3$ in (electro)catalytic studies, and tracing its source to $N_2$, require careful control experiments coupled with a healthy dose of the chemist's skepticism. The literature appears to be replete with erroneous reports.[11,12,13]

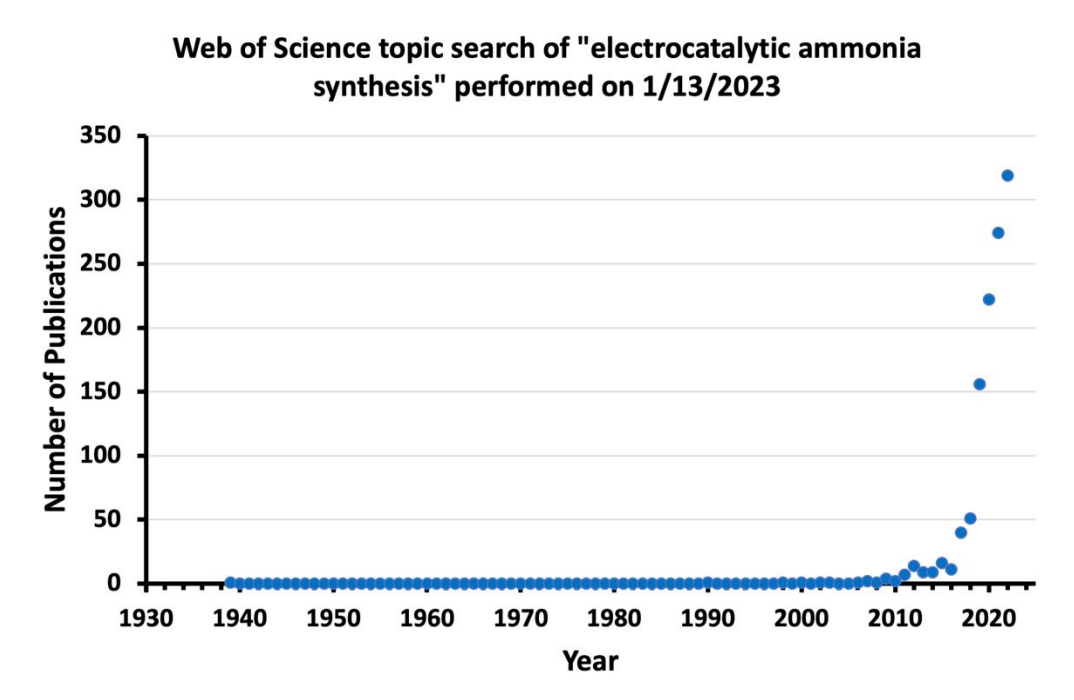**Web of Science topic search of "electrocatalytic ammonia synthesis" performed on 1/13/2023**

Figure 1. Data from the Web of Science showing the rapid growth in the number of research publications related to "electrocatalytic ammonia synthesis", as of 1/30/2023.

This caution notwithstanding, a number of studies, for example those emphasizing lithium electrodes for ammonia electrosynthesis in non-aqueous solution (e.g., THF), are robust (Figure 2).[14,15,16,17] While for lithium electrodes the energetic input to achieve ammonia electrosynthesis is significant owing to the $Li^+/Li^0$ couple, product selectivity for $NH_3$ can be high – indeed, remarkably so at moderately elevated pressures (e.g., 15 bar) with judicious choice of electrolyte salt (e.g., lithium bis(triflimide), $LiNTf_2$). A host of factors, such as avoiding the need for sacrificial organic solvent oxidation in the system, and demonstrating robust electrocatalytic cycling, still challenge the practical feasibility of these Li-based approaches.
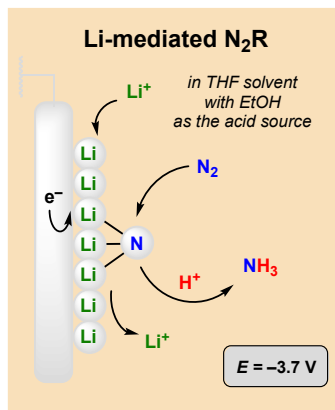
Figure 2. Schematic of Li-mediated $N_2RR$. The $Li^{0/+}$ redox potential of −3.7 V vs $Fc^{0/+}$ (the ferrocenium/ferrocene couple) was determined by MacFarlane and coworkers.[18]

Independent of these heterogeneous studies, inorganic chemists have for decades pursued coordination complexes as mechanistically well-defined catalysts for $N_2R$ via the combination of $N_2$ and H-atom equivalents (Figure 3),[19] the latter derived from reducing agents (as a source of electrons) and acids (as protons). These studies have largely been conducted under otherwise ambient conditions (room temperature or lower; 1 atm $N_2$), and benefit from a long history in applying robust analytical techniques to detect and quantify $NH_3$ (and also hydrazine, $N_2H_4$) via careful accounting for overall stoichiometry and efficiency. Early work from Chatt and coworkers paved the way.[20] A critical issue in pursuing such catalysts has been to define reductant/acid pairs that are slow to release $H_2$ under the reaction conditions.[21] The hydrogen evolution reaction (HER) is a parasitic reaction that limits the overall efficiency for conversion of electrons to fixed N product. As $H_2$ is thermodynamically accessible under most of the conditions studied, kinetic selectivity for $NH_3$ (or $N_2H_4$) is a critical issue to consider. Fortunately, a number of systems, especially those featuring Mo and Fe, have been very thoroughly studied by now (Figure 2) and provide a rich body of literature to serve as a guide.[19,21,22,23]
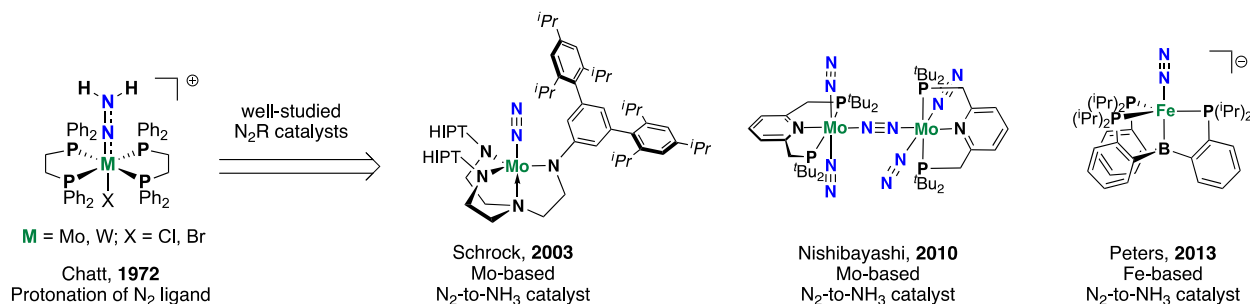


Figure 3. Representative Mo and Fe systems discussed in the text.

In terms of $N_2R$ electrocatalysis using well-defined coordination complexes, it would seem straightforward to swap a chemical reducing agent by an electrode (e.g., glassy carbon). However, putting such a plan into practice has proven challenging. Turnover limiting redox couples are most typically too cathodic; at such potentials electrode-mediated HER dominates, masking the underlying $N_2R$ that might otherwise occur. Of course, this same issue arises using catalytic electrodes in heterogeneous catalysis; background, electrode-driven HER typically dominates.[24]

## PROGRESS TOWARDS $N_2R$ ELECTROCATALYSIS USING MOLECULAR SYSTEMS

Early progress towards electrolytic (but not catalytic) $NH_3$ generation was demonstrated in a 1985 study by Pickett and coworkers that also underscored the aforementioned challenges (Figure 4).[25] Using a bis(diphenylphosphinoethane)tungsten (abbreviated as **W**) system, they showed that the hydrazido complex (TsO)**W**(NNH$_2$)$^+$ (TsO = tosylate), generated via double protonation of the bis-$N_2$ adduct *trans*-**W**(N$_2$)$_2$ by tosic acid (TsOH), released $NH_3$ (0.21 equiv $NH_3$ per **W**) upon application of a highly reducing potential (−2.6 V vs Fc$^{0/+}$; this reference is used throughout) on a Hg-pool electrode in THF; *NH$_3$ was only observed in the absence of acid*. Attempts to render this system catalytic, or to produce super stoichiometric amounts of $NH_3$ via manual cycling, proved unsuccessful. Strategies were needed to mitigate background HER by the electrode (or HER mediated by **W**) using catalysts that otherwise show appreciable kinetic selectivity for $N_2R$.
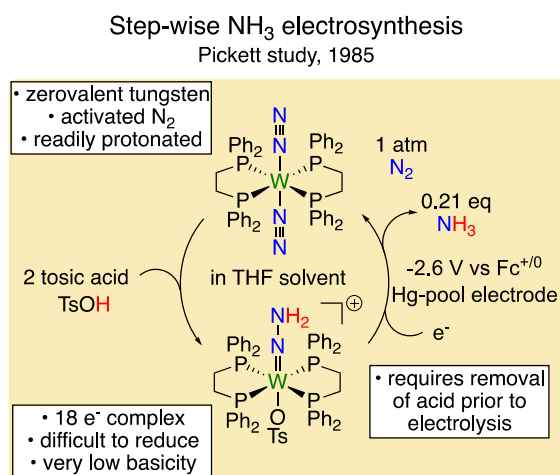
Step-wise NH$_3$ electrosynthesis
Pickett study, 1985



Figure 4. Summary of Pickett's 1985 study demonstrating step-wise (i) protonation and then (ii) electrolysis to release some $NH_3$ electrolytically.

Our lab revisited this challenge using a tris(phosphine)borane iron system that we had previously shown was capable of catalytic $N_2R$ using chemical reagents as the source of both electrons and protons.[26] A surprising but valuable lesson we had learned from our initial studies was that, at low temperature (e.g., –78 °C) in a relatively non-polar solvent such as $Et_2O$, a reductant as powerful as $KC_8$ (–3 V) is comparatively slow to reduce the strong acid $[(Et_2O)_2H][BAr^F_4]$ ($Ar^F_4$ = 3,5-$(CF_3)_2$-$C_6H_3$). As such, appreciable catalytic selectivity for $NH_3$ (~45% efficiency) compared to $H_2$ could be demonstrated.[23,26] This result suggested to us that it should be feasible to use a carbon-based electrode to drive $N_2R$ using this iron (and likely other metal) catalyst systems.

Our first evidence supporting this hypothesis was furnished in a 2016 mechanistic study of a series of $P_3^XFe$–$N_2$ complexes (X = B, C, Si).[26] Using $P_3^BFe^+$ as a precatalyst (which converts to $P_3^BFe$–$N_2$ at ~ –1.4 V) and assuming a catalytically limiting redox potential of –2.2 V vs $Fc^{0/+}$ (measured in a cold $Et_2O$ solution; measured as –2.1 V in THF at RT) corresponding to the $P_3^BFe$–$N_2^{0/-}$ couple, we were able to verify the production of up to 2.2 equiv of $NH_3$ (per Fe) by holding an applied potential at –2.3 V in the presence of 50 equiv $[(Et_2O)_2H][BAr^F_4]$ as the acid source (on a reticulated vitreous carbon working electrode in $Et_2O$ at –45 °C).

We soon thereafter learned anilinium acids could instead be used to drive $N_2R$ using $P_3^BFe$ (here using $P_3^BFe^+$ as the precatalyst) when partnered with decamethylcobaltocene ($Cp^*_2Co$) as the reductant,[27] and in 2018 were able to more firmly verify a catalytic amount of $NH_3$ (2.6 ± 0.3 equiv) could be electrocatalytically produced on a glassy carbon electrode held at -2.1 V using $[Ph_2NH_2][OTf]$ as the acid (OTf = triflate), in $Et_2O$ at –35 °C with $NaBAr^F_4$ as the electrolyte (owing to its solubility in $Et_2O$) (Figure 5).[28] As expected, the catalytic enhancement in current coincides with the $P_3^BFe$–$N_2^{0/-}$ redox couple. Interestingly, the addition of a stoichiometric equiv of $Cp^*_2Co^+$ (with respect to Fe) enhanced the $NH_3$ yield (4.0 ± 0.6 equiv per Fe; 28% FE). Also of note, chemically driven catalysis under highly comparable conditions (–35 °C with added 0.1 M $NaBAr^F_4$ in $Et_2O$, using $Cp^*_2Co$ and $[Ph_2NH_2][OTf]$) performed sworse; appreciably more $NH_3$ was produced electrocatalytically under comparable conditions.
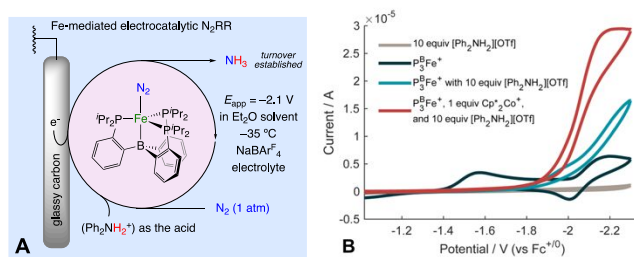


Figure 5. Reproduced in part with permission from ref 28. Copyright 2018 American Chemical Society. A: Summary of key features of $N_2R$ electrocatalysis

mediated by the $P_3^BFe(N_2)$ system. B: Cyclic voltammograms color-coded to the inset legend, demonstrating an electrocatalytic wave (red) in the presence of 10 equiv $Ph_2NH_2^+$ acid and 1 equiv each of $P_3^BFe^+$ and $Cp*_2Co^+$. Voltammograms were collected in 0.1 M $NaBAr^F_4$ solution in $Et_2O$ at −35 °C using a glassy carbon working electrode, and externally referenced to the $Fc^{+/0}$ couple. Scan rate is 100 mV/s.

## THERMODYNAMIC CONSIDERATIONS FOR ELECTROCATALYTIC N$_2$R

While gratifying as a proof of concept, the results summarized above for the $P_3^BFe$-system leave much room for improvement in terms of electrocatalysis. The bulk electrolyses are sluggish owing to the necessity of working in diethyl ether solvent at low temperature, turnover is low, and the applied potential ($E_{applied}$) needed to produce quantifiable product is more cathodic than desired. The latter issue of course limits the overall thermodynamic efficiency of the process.

Expanding on the last point, one can assess the thermal efficiency of the N$_2$R electrocatalysis by estimating the overpotential $\eta$. The use of $Et_2O$ as the working solvent compromises this analysis to an extent (thermal parameters in MeCN are more readily available), but it still proves an informative exercise. The overpotential of the system can be expressed according to equations 1 and 2, where eqn 1 describes the standard state thermodynamic potential for the reduction of N$_2$(g) by solvated acid (in MeCN) to produce two equiv of dissolved NH$_3$ in MeCN; eqn 2 then defines the overpotential relative to some $E_{applied}$.[29] For instance, consider a hypothetical example. Using a weak acid such as $Et_3NH^+$ (p$K_a$ in MeCN = 18.8) provides an $E^0$ of −1.07 V for the 6-electron process (values in eqn 1 and 2 are referenced to $Fc^{+/0}$), and a corresponding standard Gibbs free energy $\Delta G^°_{NH3,\ MeCN}$ = 74 kcal/mol. Of course, the potential needed to drive the process at an observable rate is typically cathodic of $E^0$ via some $E_{applied}$. If one could hypothetically drive N$_2$-to-NH$_3$ conversion using a common strong reductant, such as $Cp*_2Co$ (−1.91 V vs $Fc^{+/0}$), paired with $Et_3NH^+$, then the overpotential $\eta$ from eqn 2 is 0.841 V. This would be the extra potential applied to drive the process, which when converted to a free energy driving force equates to 58.2 kcal per mol NH$_3$ produced, or ~ 19 kcal per mol of electrons transferred for this hypothetical case.

$$E^0_{(N2/2\ NH3)} = 0.04\ V - 0.059(pK_a)\ \text{(eqn 1)}$$

$$\eta_{(N2/2\ NH3)} = 0.04\ V - 0.059(pK_a) - E_{applied}\ \text{(eqn 2)}$$

Our 2018 study exploited a much stronger acid, $[Ph_2NH_2]^+$ (p$K_a$ = 5.97 in MeCN), driven at an $E_{applied}$ of −2.1 V (−35 °C), to demonstrate *bona fide*

7

electrocatalysis. As the $pK_a$ of $NH_3$ (to generate $NH_4^+$) is 16.5 in MeCN, a further protonation step must therefore also be accounted for ($N_2 + 8 H^+ + 6 e^- \rightarrow 2 NH_4^+$), causing a substantial anodic shift in $E^0$ by 365 mV and a corresponding larger $pK_a$ dependence (because the number of protons is now greater than number of electrons transferred), as given in eqn 3. Plugging the needed values now provides a large η value of 2.0 V, and a corresponding driving force of 138 kcal per mol $NH_4^+$ produced, or ~46 kcal per mol of electrons transferred (note: value is not adjusted for temperature); substantial driving force is hence gained in using a stronger acid that drives $NH_4^+$ instead of $NH_3$ formation.[29]

$$\eta_{(N2/2\ NH4+)} = 0.361\ V - 0.079(pK_a) - E_{applied}\ (eqn\ 3)$$

While new strategies for HER mitigation are desired (*vide infra*), the success of these initial electrocatalysis experiments provides a valuable lesson. Comparatively strong acids expose a relatively large potential window under which $N_2R$ electrocatalysis (producing $NH_4^+$) can be observed, at least on a carbon-based electrode where background $H^+$ reduction is inoperative or sluggish,[30] especially at low temperature. A strength of the early phosphine-supported Mo and W complexes of Chatt and coworkers, the later pincer-chelated Mo systems developed by the Nishibayashi lab,[31,32] as well as our lab's phosphine-supported iron systems, is that they are comparatively stable to stronger acids, providing attractive candidates for $N_2R$ electrocatalysis studies. This contrasts the triamido(amine)-Mo systems of Schrock and coworkers,[21] which are subject to rapid degradation via protonolysis at the amides by stronger acids.

## MEDIATORS FOR ELECTROCATALYTIC PROTON-COUPLED ELECTRON TRANSFER

The above discussion summarizes some promising initial experiments in support of $N_2R$ electrocatalysis mediated by coordination complexes, with $P_3^BFe$ constituting our first line of attack. Shortcomings of the approach are nevertheless evident. The driving force needed to observe catalysis, largely a matter of necessity owing to the limiting $P_3^BFe-N_2^{0/-}$ redox couple, requires a strong applied bias (–2.1 V in the aforementioned experiment) which, for the acid used ($pK_a$ 5.97 in MeCN), leads to substantial background HER. This then limits both the thermal efficiency and selectivity of the system. It's indeed remarkable that a FE > 25% for $NH_3$ (following a free-base protocol) can be achieved under the conditions discussed above, even at –35 °C. Additionally, the $N_2R$ electrocatalysis is relatively sluggish, reflecting a multi-electron and proton transfer process occurring in a non-polar solvent ($Et_2O$) at –35 °C, with only a modest amount of $NaBAr^F_4$ supporting electrolyte (0.1 M; solubility is

limited). The demonstrated turnover number (TON) via bulk electrolysis experiments is also very modest.

Although some of these issues might be improved upon via engineering – a higher surface area electrode might for example afford higher current density and a better TON – it is the chemistry issues challenging the system that have been of primary interest to us. For the $P_3^BFe–N_2$ system, an electron transfer (ET) (–2.2 V in $Et_2O$ at low T) followed by proton transfer (PT) pathway generates the first $P_3^BFe(N_2H)$ intermediate, and a relatively strong acid (p$K_a$ lower than ~ 14 in THF (see endnote 33 for assumptions) appears to be needed to protonate anionic $P_3^BFe-N_2^-$. This situation invariably leads to substantial background HER at the electrode, and likely catalyzed HER by the iron complex as well. A proton first pathway (PT–ET) might afford a way around this issue, allowing a much weaker reductant to be employed (Schrock's Mo–system is thought to proceed this way),[19] but zerovalent $P_3^BFe–N_2$ (*note:* ignoring any boratrane backbond with respect to valence descriptors herein for simplicity) is not sufficiently basic for such a strategy to be feasible. One can shift to a system with a more cathodic limiting potential to enhance the $N_2R$ rate despite the corresponding penalty in thermodynamic driving force. However, the expected linear free energy relationship between the cathodic shift in $E^0$, the corresponding degree of $N_2$ activation, and a higher $N_2R$ rate comes with a corresponding increase in the HER rate at the electrode. The same dilemma arises by instead shifting to stronger acids. We therefore wondered whether a change in mechanism, via a proton-coupled electron transfer (PCET) pathway,[34,35,36,37] might instead prove a more effective strategy (Figure 6).
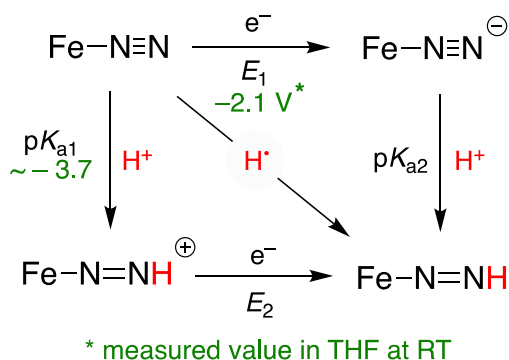


* measured value in THF at RT

Figure 6. Square Scheme for PCET pathway to deliver a net H–atom to $P_3^BFe–N_2$, showing step-wise ET–PT pathways along the edges versus a PCET pathway along the diagonal.

Traversing the diagonal from $P_3^BFe-N_2$ is appealing. For a transformation involving multiple electron/proton transfers to reduced $N_xH_y$ intermediates/products there can be thermal advantages to operating at a redox couple anodic of $P_3^BFe-N_2^{0/-}$, but this is it not trivial to achieve; reagents

that might transfer a net H-atom to $P_3^BFe-N_2$ to produce $P_3^BFe(N_2H)$, whose N–H bond dissociation free energy ($BDFE_{N-H}$) is estimated to be ≤31 kcal/mol,[27,38] aren't readily available. Although we have shown that ring-protonated decamethylcobaltocene, Cp*(*exo/endo*-$\eta^4$-$C_5Me_5H$)Co$^+$, a species likely formed in situ during catalysis driven by Cp*$_2$Co with anilinium acids, has a similarly weak $BDFE_{C-H}$,[39] Cp*$_2$Co, and its less reducing congener Cp$_2$Co, is itself a competent HER catalyst and short-circuits the system (Figure 7).[40] The primary issue for this reductant/acid pair with respect to serving as a PCET shuttle during electrocatalysis is that once the Cp-ring is protonated, which is comparatively slow, the resulting diene ligand is a good pi-acid. Its one-electron redox couple is consequently shifted anodically by more than a volt. This in turn leads to rapid reduction to Cp(CpH)Co(I), which is rather hydridic (for comparison, the $\Delta G°_{H^-}$ value of Cp*(*exo*-$\eta^4$-$C_5Me_5H$)Co is estimated to be less than 41 kcal/mol from experimental data, and is calculated to be 37 kcal/mol[39]) and leads down an HER pathway.
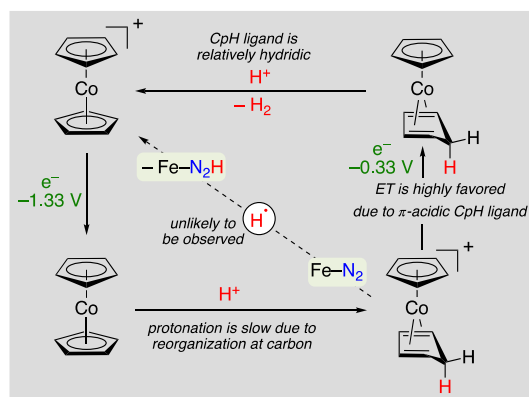


Figure 7. Cobaltocene is inefficient as a PCET mediator owing to facile HER catalysis.

To decouple the effects of protonaton and reduction of the cobaltocene, we opted to tether a Brønsted base via installation of a para-substituted dimethylaniline group off of one of the cobaltocene Cp rings, reasoning such a strategy would sufficiently insulate the protonation site from the cobalt redox center, thereby mitigating cobaltocene-mediated HER. This turned out to be an effective strategy;[40] the modified cobaltocene (Figure 8, left panel), abbreviated herein in its Co(III) unprotonated form as **Co**(III,N)$^+$, exhibits a reversible one-electron redox couple even at 10 mV s$^{-1}$ in the presence of $^{4-CN}$PhNH$_3^+$ acid (p$K_a$ 7 in MeCN) in DME. By contrast, Cp$_2$Co exhibits a catalytic HER wave under the same conditions, even at a much faster scan rate. Further ET (or PT) to **Co**(II,NH)$^+$ is not feasible. Hence, despite HER still being thermodynamically favorable (**Co**(II,NH)$^+$ features a reported N–H BDFE of 39 kcal/mol, or 37 kcal/mol when using a recently updated $C_g$ gas constant value of 52.6

kcal/mol in MeCN;[36] we use 37 kcal/mol in Figure 8 and hereafter; species with values below ~52 kcal/mol are thermally competent to release $H_2$), the only viable path for $H_2$ release would appear to be a bimolecular step bringing two cationic charges together, via a transition state whose kinetic viability is unclear.
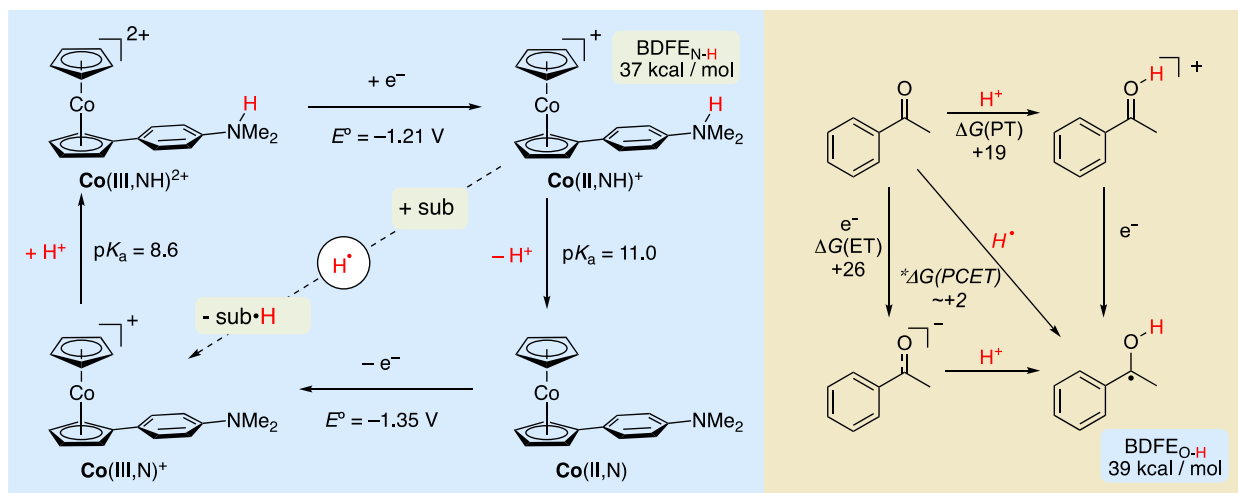


Figure 8. Left panel: Measured redox potential and p$Ka$ data for the **Co** mediator discussed, illustrating the concept of its use to deliver an H-atom via PCET to a substrate (sub) along the diagonal. Right panel: Estimated thermodynamic data for protonation first and ET first pathways for acetophenone, versus a nearly thermoneutral PCET pathway along the diagonal with respect to reaction with the (**Co**(II,NH)$^+$ form of the mediator (BDFE$_{N-H}$ and BDFE$_{O-H}$ are about 37 and 39 kcal/mol, respectively. *The BDFE$_{N-H}$ shown here is 37 kcal/mol instead of 39 kcal/mol due to the recently revised $C_g$ value of 52.6 kcal/mol in MeCN).[36]

While mitigating HER is necessary, it is not sufficient. If the modified cobaltocene system is to be useful for reductive electrocatalysis, it must mediate desired PCET steps as well. To explore this possibility, we chose acetophenone as an initial model substrate, as we estimated the O-H BDFE of the ensuing α-radical intermediate to be very well matched with the predicted BDFE of the reduced, protonated form of the mediator (37 kcal/mol; Figure 8, right panel). Moreover, step-wise protonation and reduction pathways could be excluded on thermodynamic grounds (estimated to be 19 and 26 kcal/mol uphill, respectively). Gratifyingly, a series of experiments showed that acetophenone can be electrocatalytically reduced to afford its pinacol coupling product, 2,3–diphenyl–2,3–butanediol, in the presence of the mediator, and at an appreciably faster rate at the applied potential than without the mediator (83% conversion of ketone starting material via controlled potential electrolysis (CPE) with mediator present, versus only 10% without the mediator, at $E_{applied}$ =

−1.3 V).[40] The available data are most consistent with a rate-determining concerted proton-electron transfer (CPET) step involving the mediator and the substrate (e.g., a significant KIE is observed but the rate is not dependent on $[H^+]$). This step generates an α-radical intermediate, which then bimolecularly couples in a fast second step to furnish the pinacol product. The catalytic onset is observed at -1.2 V, the same potential at which **Co**(III,NH)$^{2+}$ is reduced; hence, the electrocatalysis is pinned to the potential of the mediator, not the one-electron reduction potential of the ketone. The mediator thereby interfaces the electrode with the acid from solution to drive reductive electrocatalysis, at a sufficiently anodic potential such that (i) electrode-mediated HER is attenuated, even with a comparatively strong acid; (ii) mediator-catalyzed HER is also attenuated; and (iii) direct substrate reduction (unmediated) is also attenuated.

While our lab continues to explore the application of this electrochemical PCET mediator (*e*PCET, or alternatively abbreviated as *e*CPET when a CPET step appears to be operative) towards the reduction of other substrates (e.g., two-electron reduction of fumarate to succinate),[41,42] the mediator itself is not kinetically competent for PCET with many substrates. This perhaps is to be expected for $N_2$ (it would be very uphill to liberate free $N_2H$) but is also true of various unsaturated organic substrates whose multi-electron/proton reductions we have canvassed. Hence, we reasoned a tandem catalysis strategy might be prudent, where a co-catalyst would carry out the business end of mediating substrate reduction steps via coordination and stabilization of substrate-bound intermediates, while the mediator would facilitate overall electrocatalysis by mediating one or more key PCET step/s directly to a metal-substrate intermediate, or to a metal center (e.g., to form a hydride) that then reacts further with a substrate. These scenarios would still pin the limiting potential of the catalysis to the redox couple of the mediator (−1.2 V; Figure 9).
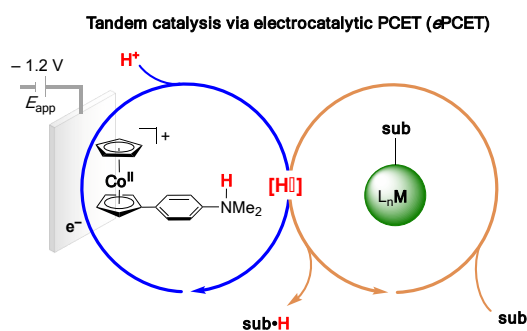


Figure 9. General scheme depicting the concept of tandem electrocatalysis via a PCET mediator. sub = substrate. −1.2 V represents the anticipated onset of electrocatalysis based on $E°$ of the cobalt mediator.

A host of multi-electron transformations would be of interest in this context, and we have begun to explore different classes. At this relatively early stage we

have learned valuable lessons from two substrates in particular (Figure 10) – $N_2$, which is the substrate of primary interest to this perspective and undergoes a net six-electron / six-proton reduction to produce $NH_3$ (or alternatively 4-electron / 4-proton to $N_2H_4$),[43] and also methyl phenylpropiolate, an alkyne substrate that can undergoe a two-electron / two proton reduction to its methyl cinnamate product (or alternatively a 4-electron / 4-proton reduction to its corresponding alkane).[44] The reduction of methyl phenylpropiolate to methyl cinnamate is summarized first, as it very clearly underscores the challenge of competitive HER, and in turn the promise of tandem catalysis via mediated PCET as a mitigation strategy.
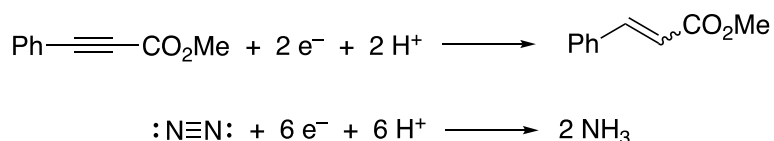
$$Ph\!\!-\!\!\!\equiv\!\!\!-\!\!CO_2Me \ + \ 2\,e^- \ + \ 2\,H^+ \ \longrightarrow \ Ph\diagup\!\!\!\diagdown\!\!\!\sim CO_2Me$$

$$:N\!\equiv\!N: \ + \ 6\,e^- \ + \ 6\,H^+ \ \longrightarrow \ 2\,NH_3$$

Figure 10. Semihydrogenation of methyl phenylpropiolate and complete reduction of $N_2$, respectively.

## Semihydrogenation of an alkyne via tandem electrocatalytic PCET

Methyl phenylpropiolate is unreactive towards tosic acid hydrate (TsOH•$H_2O$; p$K_a$ 8.6 in MeCN) and is not competently reduced on a carbon-based electrode, including boron-doped diamond (BDD), a form of carbon that is less efficient at HER than glassy carbon. We wondered whether a prototypical HER catalyst might be redirected to methyl phenylpropiolate reduction using a BDD electrode, and chose to study the Ni-based HER catalyst (dmpe)$_2$Ni$^{2+}$ (dmpe = bis(dimethylphosphino)ethane) as a prototype. Of course, use of an acid as strong as TsOH•$H_2O$ might pose the challenge of competing HER at the turnover limiting redox potential, but since (dmpe)$_2$Ni$^{2+}$ is reduced at potentials below –1.6 V in MeCN to (dmpe)$_2$Ni(0), and since BDD does not efficiently catalyze HER at this potential,[30] it might be reasonably deduced that TsOH•$H_2O$ would competitively protonate (dmpe)$_2$Ni(0) to furnish (dmpe)$_2$Ni(H)$^+$; the latter intermediate might then be capable of delivering a hydride to the alkyne substrate. This doesn't turn out to be the case, however. TsOH•$H_2O$ is too strong an acid and an onset for HER occurs at about –1.6 V (Figure 11A). Thus, while electrode-catalyzed HER is significantly attenuated at this potential on BDD (evident from the available CV data), Ni-catalyzed HER is too highly favored under the conditions. Hence, for this system one faces the dual challenge of mitigating the background HER from the electrode and also catalyzed HER by (dmpe)$_2$Ni$^{2+}$.

If during the catalyzed HER cycle protonation of (dmpe)$_2$Ni(H)$^+$ (to liberate $H_2$ and (dmpe)$_2$Ni$^{2+}$) is the central problem to overcome, one might employ an acid that is capable of protonating (dmpe)$_2$Ni(0) to furnish (dmpe)$_2$Ni(II)(H)$^+$, but too weak to protonate (dmpe)$_2$Ni(II)(H)$^+$. Benzoic acid (p$K_a$ 22) satisfies these

criteria, but does not give rise to effective reduction of methyl phenylpropiolate; HER still dominates.[44] The dilemma within this nickel system is that $(dmpe)_2Ni(II)(H)^+$ is readily reduced to the nickel(I) hydride, $(dmpe)_2Ni(I)(H)$, at −1.4 V; the latter Ni(I) species is *very* hydridic ($\Delta G°_H^- = 27.2$ kcal/mol) and thus is rapidly protonated even by benzoic acid. Whether using an acid as strong as TsOH•$H_2O$, or as weak as benzoic acid, at an $E_{applied}$ significantly below −1.4 V the $(dmpe)_2Ni(I)(H)$ intermediate predisposes the system's selectivity towards HER.

The cobalt PCET mediator provides a means to infiltrate the HER wall. When it is additionally added to the solution, along with the substrate, TsOH•$H_2O$, and $(dmpe)_2Ni^{2+}$, electrocatalytic reduction of methyl phenylpropiolate turns on (Figure 11A,B). All the components are essential to the electrocatalysis, intimating a tandem catalytic process. Based on mechanistic data available it is evident that a turnover limiting PCET step from **Co**(II,NH)$^+$ to $(dmpe)_2Ni(II)^{2+}$ produces a nickel(III) hydride, $(dmpe)_2Ni(III)(H)^{2+}$ (releasing **Co**(III,N)$^+$ as the byproduct).[44] $(dmpe)_2Ni(III)(H)^{2+}$ is very readily reduced to $(dmpe)_2Ni(II)(H)^+$ ($E_{1/2}$ estimated to be about -0.15 V) at the potential of the mediator (−1.2 V), but not to $(dmpe)_2Ni(I)(H)$. Hence, $(dmpe)_2Ni(II)(H)^+$ can be intercepted by the alkyne substrate (in preference to the TsOH•$H_2O$ that is also present) to provide the semihydrogenated product (Figure 12). Critically, operating at the mediator's potential of −1.2 V provides access to $(dmpe)_2Ni(II)(H)^+$ while avoiding $(dmpe)_2Ni(0)$ and $(dmpe)_2Ni(I)(H)$. A desired 2 e$^-$/ 2 H$^+$ reductive electrocatalytic process is thereby exposed because the catalytic HER shunt pathway is closed off. Applying the PCET mediator towards the 6 e$^-$/ 6 H$^+$ reduction of $N_2$ illustrates a similar principle.
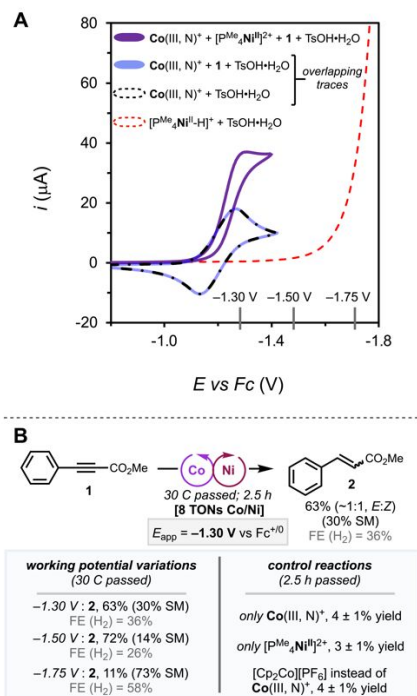
Figure 11. Reproduced with permission from ref 44. Copyright 2022 American Chemical Society. A: CVs corresponding to color coded inset legend. CV conditions: 1 mM Co(III, N)$^+$, 5 mM [P$^{Me}_4$Ni$^{II}$]$^{2+}$, 25 mM methyl phenylpropiolate, 50 mM TsOH•H$_2$O, 75 mM [TBA][NTf$_2$] using a BDD disk working electrode and GC disk counter electrode. B: CPE for selective conjugate reduction of methyl phenylpropiolate under tandem electrocatalytic conditions, at various potentials, and control reactions. CPE conditions: 3 mM Co(III, N)$^+$, 3 mM [P$^{Me}_4$Ni$^{II}$]$^{2+}$, 37.5 mM **1**, 225 mM TsOH•H$_2$O, 75 mM [TBA][NTf$_2$], BDD(–)/Zn(+) with a Ag/AgOTf reference electrode in a divided cell.
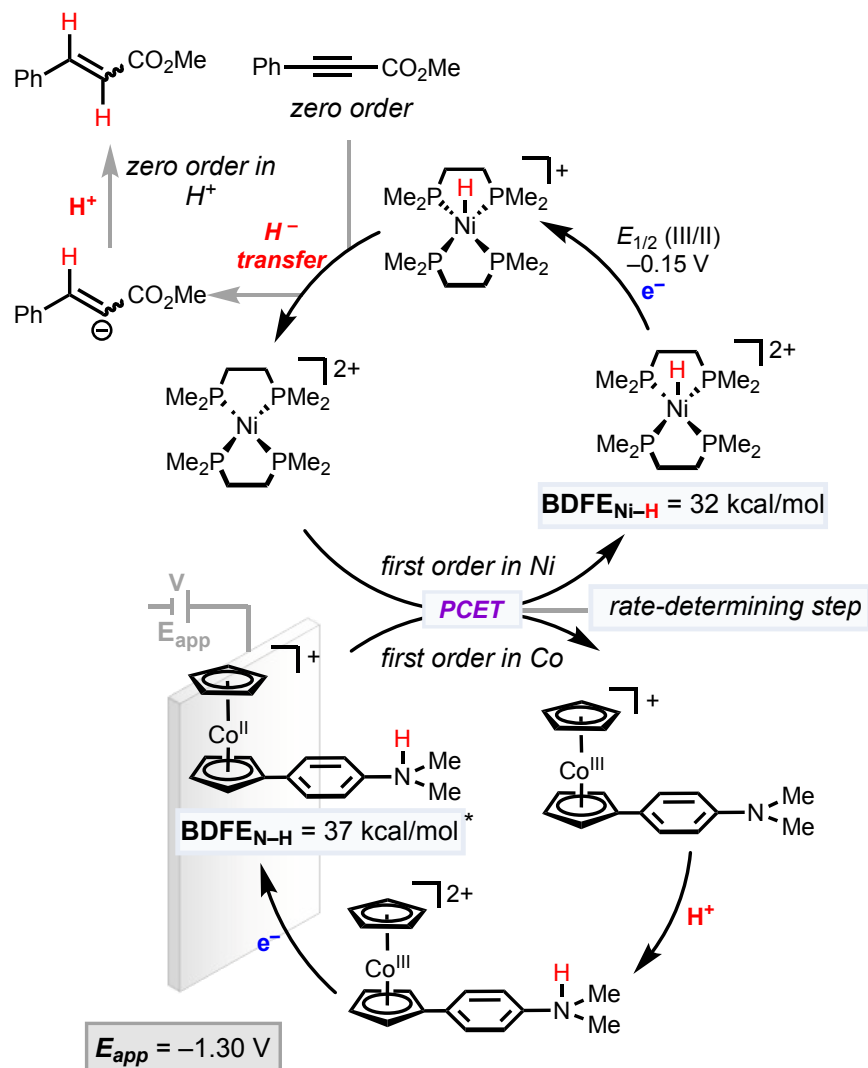
Figure 12. Favored mechanistic pathway accounting for the semihydrogenation of methyl phenylpropiolate via PCET-mediated tandem reductive electrocatalysis. *See above for discussion of this updated BDFE$_{N-H}$ value.

## Complete hydrogenation of N$_2$ via tandem electrocatalytic PCET

Returning to Chatt and Pickett's (TsO)**W**(NNH$_2$)$^+$ system, we wondered whether it might be rendered an electrocatalyst for N$_2$RR in the presence of the **Co**(III,N)$^+$ mediator, using the same acid (TsOH•H$_2$O) Pickett had explored (*vide supra*). Worth noting for this **W** system is that its zerovalent form, *trans*-**W**(N$_2$)$_2$, is rapidly and quantitatively converted to (TsO)**W**(NNH$_2$)$^+$ in the presence of excess TsOH•H$_2$O. On loading a solution with either *trans*-**W**(N$_2$)$_2$ or (TsO)**W**(NNH$_2$)$^+$ in the presence of TsOH•H$_2$O and **Co**(III,N)$^+$ the only **W** species present is (TsO)**W**(NNH$_2$)$^+$; this therefore is the (pre)catalyst state prior to

application of an electrochemical potential; one expects two (relatively) efficient on-path protonation steps to be operative on cycling through *trans*-$\mathbf{W}(N_2)_2$ to form $(TsO)\mathbf{W}(NNH_2)^+$. Since $(TsO)\mathbf{W}(NNH_2)^+$ is a closed-shell 18-electron complex it is not readily, nor reversibly, reduced. An applied bias cathodic of –1.9 V is needed to drive a reductive process in the presence of $TsOH \cdot H_2O$ at a BDD electrode (using THF as solvent and 0.1 M $[Li][NTf_2]$ as electrolyte); electrode-mediated HER dominates well anodic of this potential (Figure 13). Hence, $N_2R$ electrocatalysis is not anticipated nor observed.
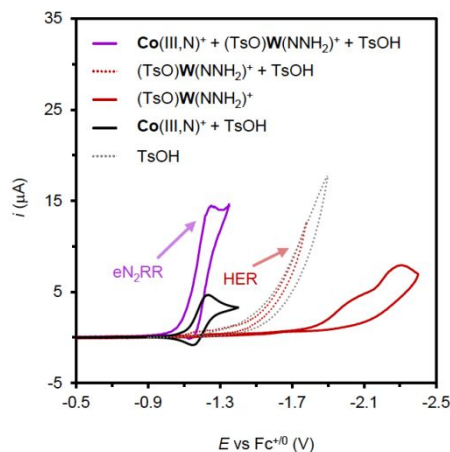


Figure 13. Reproduced with permission from ref 43. Copyright 2022 Springer Nature. CV data reproduced for the $(TsO)\mathbf{W}(NNH_2)^+$ $N_2R$ tandem electrocatalyst system. CV of 50 mM $TsOH \cdot H_2O$ (dashed grey); 0.5 mM $\mathbf{Co}(III,N)^+$ with 50 mM $TsOH \cdot H_2O$ (black); 0.5 mM $(TsO)\mathbf{W}(NNH_2)^+$ (solid red); 0.5 mM $(TsO)\mathbf{W}(NNH_2)^+$ with 50 mM $TsOH \cdot H_2O$ (dashed red); 0.5 mM $\mathbf{Co}(III,N)^+/(TsO)\mathbf{W}(NNH_2)^+$ with 50 mM $TsOH \cdot H_2O$ (purple). CVs were performed at 100 mV·s$^{-1}$ in 0.1 M $[Li][NTf_2]$ THF solution using a BDD disk as the working electrode, Pt disk as the counter electrode and Ag/AgOTf (5 mM) as the reference electrode.

Things get more interesting on addition of $\mathbf{Co}(III,N)^+$.[43] Now, an electrocatalytic wave coincident with the mediator's potential is observed (Figure 13, purple trace), and CPE at -1.35 V (in DME, 1 atm $N_2$, 25 °C) confirms production of ~ 11.5 equiv $NH_3$ per $(TsO)\mathbf{W}(NNH_2)^+/\mathbf{Co}(III,N)^+$, with a FE of ~ 45% (averaging several runs; note that some $NH_3$ is oxidized at the counter-electrode used, so 45% FE represents a *lower limit*; 40 equiv $NH_3$ were instead produced at 43% FE by using a larger surface area GC foam electrode). An exhaustive set of control experiments establishes $N_2$ as the sole source of the $NH_3$ produced, and a number of mechanistic experiments point to a concerted PCET step from $\mathbf{Co}(II,NH)^+$ to $(TsO)\mathbf{W}(NNH_2)^+$ with a modest rate (~ 0.5 s$^{-1}$) as rate-contributing, consistent with the rather slow electrocatalytic rate overall. It is also observed that the addition of two equiv $\mathbf{Co}(II,N)$ to a mixture of $(TsO)\mathbf{W}(NNH_2)^+$ with excess $TsOH \cdot H_2O$ present liberates $NH_3$ over a few hours (note: no $NH_3$ is

released without added **Co**(II,N)). The only new **W** species present at the end of this reaction is (TsO)**W**(NH)$^+$, which we suggest results following PCET to (TsO)**W**(NNH$_2$)$^+$ with NH$_3$ loss and N-N cleavage to produce (TsO)**W**(N)$^+$ (Figure 14); the latter should be easily reduced to (TsO)**W**(N), which can then be protonated to produce (TsO)**W**(NH)$^+$; (N$_3$)**W**(N) can alternatively be used as a precatalyst in the electrocatalytic process, consistent with (TsO)**W**(N) being a viable intermediate. Some (TsO)**W**(NNH$_2$)$^+$ is also present at the end of the chemically driven reaction, suggesting the system cycles through to produce a second equiv of NH$_3$ from (TsO)**W**(N), presumably followed by rebinding of N$_2$ to produce *trans*-**W**(N$_2$)$_2$, the precursor to (TsO)**W**(NNH$_2$)$^+$ via protonation by the excess acid present. While the mechanism shown in Figure 14 is a reasonable hypothesis it will be interesting to try to further tease this system apart, and to identify which steps may be step-wise PT-ET versus PCET throughout the cycle.
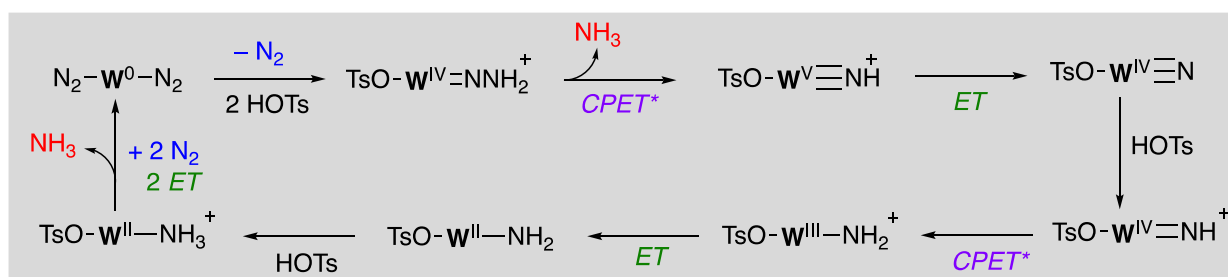


Figure 14. One plausible catalytic cycle by which TsO**W**=NNH$_2^+$ serves as an on-path intermediate of tandem N$_2$RR electrocatalysis in the presence of the PCET mediator. Note that some intermediates shown, and steps, remain ill-defined, such as the cycling of TsO**W**(NH$_3$)$^+$ to *trans*-**W**(N$_2$)$_2$ with liberation of NH$_3$, requiring in net two electrons and two molecules of N$_2$. *For these PCET steps we favor concerted proton electron transfer (CPET) based on reasonable estimates of the observed catalytic rate from measured data and a corresponding analysis of the feasibility (or lack thereof) of $k_{reverse}$ for step-wise ET-PT or PT-ET pathways, based on thermodynamic data, as discussed in Section 13 of the Supporting Information of reference 43.

The above results are intriguing in terms of thermal efficiency and selectivity. In the original Pickett study the release of any degree of NH$_3$ from (TsO)**W**(NNH$_2$)$^+$ using TsOH•H$_2$O as the acid source in THF required an $E_{applied}$ cathodic of –2.6 V. Application of eqn 3 above (N$_2$ / 2 NH$_4^+$) provides a corresponding overpotential η of 2.28 V, or 158 kcal/mol NH$_4^+$.  With the PCET mediator present, onset of catalysis with the same acid occurs at –1.2 V, with *bona fide* electrocatalysis operative, at an η of 880 mV, or 61 kcal per mol NH$_4^+$. The difference in thermodynamic efficiency is striking. Regarding selectivity, the system can be compared to an aforementioned study from MacFarlane and coworkers using a Li$^+$/Li electrode system and [Li][NTf$_2$] as a privileged electrolyte. While they were able to demonstrate near quantitative

conversion of $N_2$ to $NH_3$ (FE ~100%) at 15 atm $N_2$ using their electrode set-up, at 1 atm $N_2$ the FE of their system dropped to ~16%. Confirmation of the viability of electrocatalytic cycling of this $Li^+$/Li electrode system (i.e., *bona fide* electrocatalysis) remains to be described. It will be of interest to study the $(TsO)\mathbf{W}(NNH_2)^+$ electrocatalyst system at higher pressures for additional comparisons with respect to selectivity.

A point of special interest to us was to consider how other inorganic complexes that are known to catalyze $N_2R$ in the presence of chemical reducing agents and acids would behave under electrocatalytic conditions in the presence of the $\mathbf{Co}(III,N)^+$ mediator. Given our present understanding of how the tandem system works, if a turnover limiting step to some $M-N_xH_y$ intermediate (e.g., an ET step followed by an uncoupled PT step) can instead be mediated by a PCET step from $\mathbf{Co}(II,NH)^+$, then there is a reasonable chance $N_2R$ electrocatalysis will be observed. If instead a strictly ET step defines the turnover limiting potential for the system, we would not expect to observe $N_2R$ electrocatalysis, or at least not at the potential of the mediator. We hence undertook studies to explore this.[43,45]

Using a small family of previously reported $N_2R$ catalysts featuring Mo, Fe, and Os (Fe and Os as reported by our lab; Mo as reported by Nishibayashi's lab; Figure 15, left panel), we studied their respective capacities to mediate electrocatalytic $N_2R$ in tandem with $\mathbf{Co}(III,N)^+$ *under the same conditions used for (TsO)$\mathbf{W}$(NNH$_2$)$^+$.*[43] Each of these complexes serves as an $N_2R$ electrocatalyst in the presence of TsOH•$H_2O$ and $\mathbf{Co}(III,N)^+$, and *at the same potential* (onset at –1.2 V; Figure 15, right panel). This is a fascinating result; despite different metals in different coordination geometries with different ligands, and different turnover limiting redox couples under non-mediated conditions using chemical reductants, a modest catalytic wave is observed in each case that is pinned to the potential of the PCET mediator. The implication is clear. So long as the PCET mediator facilitates a PCET step that bypasses a turnover limiting redox couple that otherwise necessitates a more cathodic potential, tandem electrocatalysis at the mediator's potential becomes feasible.
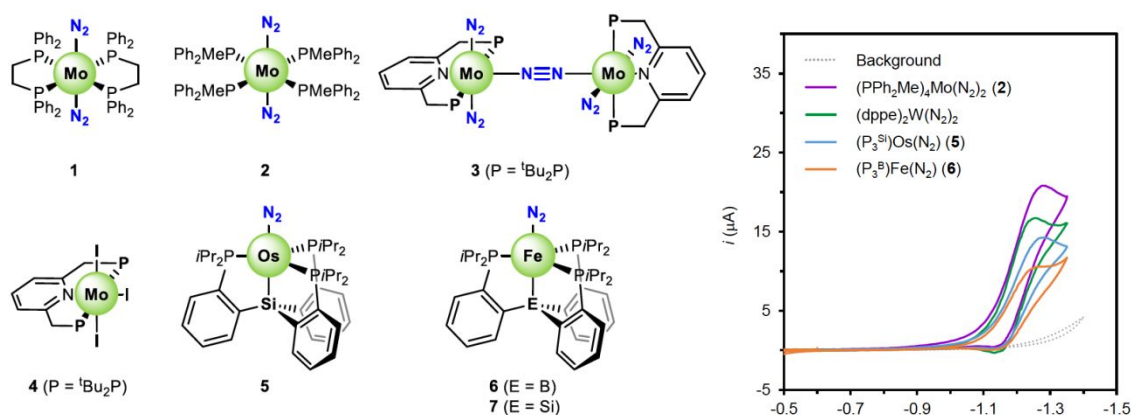
Figure 15. Reproduced with permission from ref 43. Copyright 2022 Springer Nature. CVs of several representative **M**$(N_2)$ catalysts studied under the standard electrocatalytic conditions in the presence of **Co**$(III,N)^+$ and TsOH, showing a multi-electron catalytic wave for $N_2$RR in each case at the same applied bias as for **W**$(N_2)_2$. **Note:** All CVs in A-F were performed at 100 mV·s$^{-1}$ (unless otherwise stated) in 0.1 M [Li][NTf$_2$] THF solution using a BDD disk as the working electrode, Pt disk as the counter electrode and Ag/AgOTf (5 mM) as the reference electrode.

Moreover, it need not be the same step of an $N_2$R cycle. For instance, in contrast to (TsO)**W**$(N_2)_2$, $P_3^B$Fe-$N_2$ is not sufficiently basic to be protonated by TsOH•H$_2$O, or even by stronger acids such as HOTf. Hence, electrochemical cycling through zerovalent $P_3^B$Fe-$N_2$ requires either an ET step (to generate $P_3^B$Fe-$N_2^-$, which can then be protonated to generate $P_3^B$Fe(N$_2$H)), or a PCET step (to generate $P_3^B$Fe(N$_2$H) directly). At the potential of the **Co**$(III,N)^+$ mediator (−1.2 V) the direct ET pathway should not be kinetically accessible. Hence, PCET from **Co**$(II,NH)^+$ to $P_3^B$Fe–$N_2$ to furnish $P_3^B$Fe(N$_2$H) (about 7 kcal/mol uphill based on estimated BDFE$_{N-H}$ values) is inferred. This iron system is additionally distinct from (TsO)**W**$(NNH_2)^+$. $N_2$ binding in the $P_3^B$Fe–$N_2$ system is most efficient in the 0 or -1 states (i.e., the $P_3^B$Fe–$N_2^{0/-}$ species); the cationic +1 state doesn't bind $N_2$ well; in THF or DME by far the primary species is the free cation $P_3^B$Fe$^+$. Hence, for this Fe system a rate-contributing ET step (at ~ −1.4 V) is needed to convert $P_3^B$Fe$^+$ to $P_3^B$Fe–$N_2$, required for the on-path PCET step to generate $P_3^B$Fe(N$_2$H) (Figure 16). As a consequence of this, the TON of the Fe system increases at a more cathodic potential (9.3 equiv NH$_3$ at −1.45 V vs 5.6 at −1.35 V); the $P_3^B$Fe–$N_2$ concentration is expected to be higher at more negative potential.
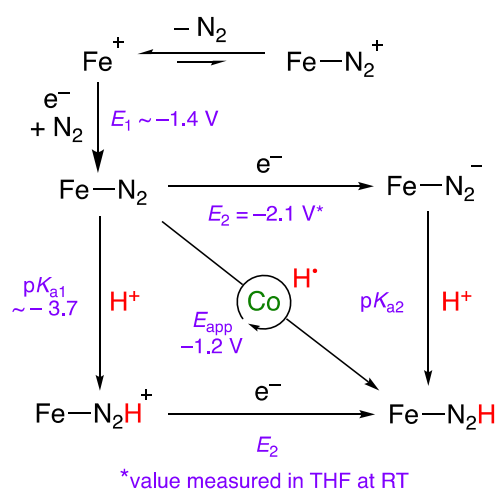


Figure 16. Mechanistic scheme providing a rationalization of the potential-dependent enhancement of $N_2$RR mediated by the $P_3^B$Fe-system, where an ET process ($E_1$) increases the availability of $P_3^B$Fe-$N_2$, the intermediate proposed to react with the cobalt PCET mediator to form $P_3^B$Fe-$N_2$H.

An interesting counter point to the above examples is Nishibayashi's [Mo(III)X$_3$($^H$PNP)] N$_2$R catalyst system ($^H$PNP = 2,6-bis(di-*tert*-butylphosphinomethyl)pyridine; X = Cl, Br, I). The on-path mechanism for these systems is proposed to feature a bimolecular N$_2$ splitting step (to form Mo(IV)X(N)($^H$PNP)) from a Mo(I) state that is accessed at a potential beyond −1.8 V. Hence, a Mo(III/II) ET step (releasing halide) at a potential well cathodic of the **Co**(III,N)$^+$ mediator is needed to drive the system forward towards N$_2$ binding and bimolecular scission. As a result, the PCET mediator is ineffective for this pre-catalyst; CPE under the same conditions at −1.35 V does not produce NH$_3$.

We have, however, found that unmediated electrocatalytic N$_2$R can be achieved in this system by careful selection of conditions (Figure 17). Hence, using collidinium triflate ([ColH][OTf]) as the acid and [MoBr$_3$($^H$PNP)] as the pre-catalyst a CPE experiment on a BDD electrode at an applied potential of −1.89 V with [Li][NTf$_2$] as the electrolyte produced 11.7 equiv NH$_3$ at 43% FE. With collidinium acid electrode-mediated N$_2$R doesn't begin until about −1.9 V and hence catalyzed N$_2$R is kinetically competitive. The overpotential η for this system is estimated at 1.1 V (or ~75 kcal per mol NH$_4^+$), with the reduction in efficiency at a much more cathodic $E_{applied}$ (compared with the mediated N$_2$R) being partly offset by use of a significantly weaker acid than tosic acid (pKa of [ColH]$^+$ is estimated at 15 in MeCN[46]).
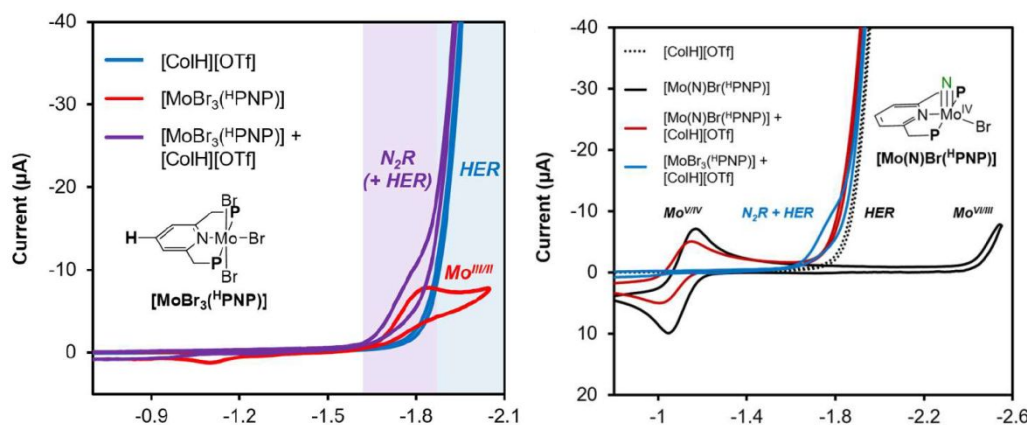


Figure 17. Reproduced with permission from ref 45. Copyright 2023 American Chemical Society. Left panel: Cyclic voltammograms of 0.5 mM [Mo] (red trace), 50 mM [ColH][OTf] (blue trace; ColH = colidinium), and 0.5 mM [Mo] with 50 mM [ColH][OTf] (purple trace) in a THF solution containing 100 mM [Li][NTf$_2$]. A BDD working electrode was employed at a 100 mV/s scan rate. Right panel: CV of [Mo(N)Br($^H$PNP)] in the presence and absence of [ColH][OTf] and comparison to just [ColH][OTf] or [MoBr$_3$($^H$PNP)] in the presence of [ColH][OTf].

## THE ROAD AHEAD

The study of electrocatalytic $N_2R$ mediated by molecular catalysts is at a very early stage but holds promise for significant advances. While this perspective emphasizes examples and progress from our own lab's work, there have been interesting studies from other laboratories in pursuit of $N_2R$ electrocatalysis via synthetic complexes.[47,48,49] We underscore that caution should be exercised in evaluating whether these and related studies (including our own of course) reliably establish electrocatalysis. As for the heterogeneous community (*vide supra*), erroneous reports of $N_2R$ electrocatalysis have been verified that serve as a sober reminder of the need for careful controls, quantification, and healthy skepticism in this sub-field.[50]

With respect to the systems described herein, a number of lessons have emerged. Foremost among them is the value of PCET-mediated electrocatalysis, and the improved thermodynamic efficiency that can be achieved for a multielectron/proton transfer process. This PCET-mediated approach has enabled a diverse family of substrates, including for example acetophenone, methyl phenylpropiolate, and $N_2$, to be electrocatalytically reduced by 1-, 2-, or 6- electrons, respectively, at a single potential (onset at $-1.2$ V) while using the same acid (and hence driving force). This is an unusual observation, and in certain regards is reminiscent of enzymatic behavior, where Nature has evolved strategies to operate on a range of substrates at a single, biologically pinned potential. Taking this analogy even further, for the tandem $N_2R$ electrocatalysis described herein, the synthetic "active sites" for $N_2R$ can accommodate a host of different transition metals, in different coordination environments, with variable associated redox couples. But the presence of the PCET mediator facilitates multielectron $N_2R$ electrocatalysis for these variously substituted "cofactors" at a single applied thermodynamic driving force. While admittedly a rough comparison, this behavior is also reminiscent of enzymes, for example $N_2$ases, where differently substituted cofactors (Mo, V, Fe) are known to mediate $N_2R$ with variable selectivity for $NH_3$ versus $H_2$ at a single (biologically accessible) thermodynamic potential.[51,52]

While this progress is encouraging, the PCET-mediated catalysis we have described operates at modest catalytic rates. Our initial approach does not, at least as yet, incorporate a purposeful design strategy for pre-organizing the substrate (or a substrate-bound metal complex) and the PCET mediator. To a first approximation, each PCET step requires encounters between freely diffusing species. In terms of catalytic function, Nature's enzymes are far more elegant in this regard as they often benefit from preorganization strategies to help achieve rapid rates at high thermodynamic efficiency (i.e., low overpotential). Future synthetic efforts to improve electrochemical PCET should therefore focus on the design of *e*PCET mediators that can achieve enhanced rates at fixed driving force via built-in chemical structures that enable a substrate (or a metal-substrate complex, or alternatively a metal complex prior

to substrate binding) to associate with the PCET mediator via a favorable pre-equilibrium before a rate-contributing PCET step. Indeed, for certain substrates we have canvassed it may be that some pre-association with the mediator is fortuitously operative. Studies are needed to explore this possibility in detail to help guide further rational design strategies.

Another area ripe with opportunity concerns the incorporation of a photochemical strategy within the PCET-mediated electrochemical catalysis. Photoelectrochemical transformations are being explored in a variety of contexts, including towards the reduction of organic substrates;[53,54] photochemically driven reductive PCET transformations are also attracting attention within the organic chemistry community.[55] The design of PCET mediators that can store a comparatively stable H-atom equivalent (with respect to $H_2$ evolution) that becomes far more reactive upon photo-excitation[56] could enable electrocatalytic $N_2R$ at much milder electrochemical potentials, where most of the driving force is translated to a photochemical potential.

While such an approach has yet to be reported for $N_2R$, a pair of recent studies, including one from our laboratory[57] and also a highly related study published very soon thereafter by Nishibayashi and coworkers,[58] have demonstrated photocatalytic $N_2$ reduction by well-defined complexes for the first time, using molybdenum $N_2R$ catalysts (of the type originally reported by Nishibayashi and coworkers for thermally driven $N_2R$) partnered with photoactive organic hydride and/or H-atom donors. While notably not required for the system that we reported,[57] an iridium photoredox catalyst facilitates the overall catalysis. It is easy to imagine, though likely not straightforward in practice, interfacing electrochemistry with such systems to achieve photoelectrochemical $N_2R$ where the spent organic donor is electrochemically recycled. Effort is worth investing towards this goal.

## ACKNOWLEDGEMENTS

Resnick Sustainability Institute at Caltech for enabling resources on Caltech's campus that have amplified the research we have been able to carry out.

[1] Smil, V. Global Population and the Nitrogen Cycle. *Sci. Am.* **1997**, *277*, 76–81.

[2] Birkeland, K. R. On the Oxidation of Atmospheric Nitrogen in Electric Arcs. *Trans. Faraday Soc.*, **1906**, *2*, 98-116.

[3] Storch, H. H.; Olson, A. R. The Synthesis of Ammonia From its Elements in the Low-Voltage Arc. *J. Am. Chem. Soc.*, **1923**, *45,* 1605-1614.

[4] Mehta, P.; Barboun, P.; Herrera, F. A.; Kim, J.; Rumbach, P.; Go, D. B.; Hicks, J. C.; Schneider, W. F. Overcoming ammonia synthesis scaling relationships with plasma-enabled catalysis. *Nat. Catal.* **2018**, *1*, 269-275.

[5] Tullo, A. H. Is Ammonia the Fuel of the Future? *Chem. Eng. News*. **2021** *99*.

[6] Wang, M.; et al. Can sustainable ammonia synthesis pathways compete with fossil-fuel based Haber–Bosch processes? *Energy Environ. Sci.* **2021**, *14*, 2535–2548.

[7] Hochman, G.; Goldman, A. S.; Felder, F. A.; Mayer, J. M.; Miller, A. J. M.; Holland, P.; Goldman, A. L.; Manocha, P.; Song, Z.; Aleti, S. Potential Economic Feasibility of Direct Electrochemical Nitrogen Reduction as a Route to Ammonia. *ACS Sustainable Chem. Eng.* **2020**, *8*, 8938-8948.

[8] MacFarlane, D. R.; et al. A Roadmap to the Ammonia Economy. *Joule* **2020**, *4*, 1186–1205.

[9] Lazouski, N.; Limaye, A.; Bose, A.; Gala, M. L.; Manthiram, K.; Mallapragada, D. S. Cost and Performance Target for Fully Electrochemical Ammonia Production under Flexible Operation. *ACS Energy Lett.* **2022**, *7*, 2627-2633.

[10] Qing, G. *et al.* Recent advances and challenges of electrocatalytic $N_2$ reduction to ammonia. *Chem. Rev.* **2020**, *120*, 5437–5516.

[11] Du, H. -L.; Hodgetts, R. Y.; Chatti, M.; Nguyen, C. K.; Macfarlane, D. R.; Simonov, A. N. Is Molybdenum Disulfide Modified with Molybdenum Metal Catalytically Active for the Nitrogen Reduction Reaction? *J. Electrochem. Soc.* **2020**, *167*, 146507-146507.

[12] Hu, B.; Hu, M.; Seefeldt, L.; Liu, T. L. Electrochemical Dinitrogen Reduction to Ammonia by $Mo_2N$: Catalysis or Decomposition? *ACS Energy Lett.* **2019**, *4*, 1053-1054.

[13] Izelaar, B. et. al. Revisiting the Electrochemical Nitrogen Reduction on Molybdenum and Iron Carbides: Promising Catalysis or False Positives? *ACS Catal.* **2023**, *13*, 1649-1661.

[14] Tsuneto, A., Kudo, A., and Sakata, T. Efficient Electrochemical Reduction of $N_2$ to $NH_3$ Catalyzed by Lithium. *Chem. Lett.* **1993**, 851–854.

[15] Tsuneto, A.; Kudo, A.; Sakata, T. Lithium-mediated Electrochemical Reduction of High Pressure $N_2$ to $NH_3$. *J. Electroanal. Chem*. **1994**, 367, 183-188.

[16] Lazouski, N.; Chung, M.; Williams, K.; Gala, M. L.; Manthiram, K. Non-aqueous gas diffusion electrodes for rapid ammonia synthesis from nitrogen and water-splitting-derived hydrogen. *Nat. Catal.* **2020**, **3**, 463–469.

[17] Du, H. -L. et. al. Electroreduction of Nitrogen with Almost 100% Current-to-Ammonia Efficiency. *Nature* **2022**, *609*, 722-727.

[18] Suryanto, et al. Nitrogen Reduction to Ammonia at High Efficiency and Rates Based on a Phosphonium Proton Shuttle. *Science*, **2021**, *372*, 1187-1191.

[19] For a recent and comprehensive review on this topic see: Chalkley, M. J.; Drover, M. W.; Peters, J. C. Catalytic $N_2$-to-$NH_3$ (or $N_2H_4$) Conversion by Well-defined Molecular Coordination Complexes. *Chem. Rev.* **2020,** *120*, 5582–5636.

[20] Chatt, J.; Dilworth, J. R.; Richards, R. L. Recent Advances in Chemistry of Nitrogen-Fixation. *Chem. Rev.* **1978**, *78*, 589–625.

[21] Yandulov, D. V.; Schrock, R. R. Catalytic Reduction of Dinitrogen to Ammonia at a Single Molybdenum Center. *Science* **2003**, *301*, 76–78.

[22] Arashiba, K.; Miyake, Y.; Nishibayashi, Y. A Molybdenum Complex Bearing PNP-Type Pincer Ligands Leads to the Catalytic Reduction of Dinitrogen into Ammonia. *Nat. Chem.* **2010**, *3*, 120–125.

[23] Anderson, J. S.; Rittle, J.; Peters, J. C. Catalytic Conversion of Nitrogen to Ammonia by an Iron Model Complex. *Nature* **2013**, *501*, 84–87.

[24] Cai, X. et al. Lithium-mediated Electrochemical Nitrogen Reduction: Mechanistic Insights to Enhance Performance. *iScience* **2021**, *24*, 103105.

[25] Pickett, C. J.; Talarmin, J. Electrosynthesis of Ammonia. *Nature* **1985**, *317*, 652–653.

[26] Del Castillo, T. J.; Thompson, N. B.; Peters, J. C. A Synthetic Single-Site Fe Nitrogenase: High Turnover, Freeze-Quench [57]Fe Mossbauer Data, and a Hydride Resting State. *J. Am. Chem. Soc.* **2016**, *138*, 5341–5350.

[27] Chalkley, M. J.; Del Castillo, T. J.; Matson, B. D.; Roddy, J. P.; Peters, J. C. Catalytic $N_2$-to-$NH_3$ Conversion by Fe at Lower Driving Force: A Proposed Role for Metallocene-Mediated PCET. *ACS Cent. Sci.* **2017**, *3*, 217–223.

[28] Chalkley, M. J.; Del Castillo, T. J.; Matson, B. D.; Peters, J. C. Fe-Mediated Nitrogen Fixation with a Metallocene Mediator: Exploring $pK_a$ Effects and Demonstrating Electrocatalysis. *J. Am. Chem. Soc.* **2018**, *140*, 6122–6129.

[29] For a thorough discussion see: Lindley, B. M.; Appel, A. M.; Krogh-Jespersen, K.; Mayer, J. M.; Miller, A. J. M. Evaluating the Thermodynamics of Electrocatalytic $N_2$ Reduction in Acetonitrile. *ACS Energy Lett.* **2016**, *1*, 698–704.

[30] McCarthy, B. D.; Martin, D. J.; Rountree, E. S.; Ullman, A. C.; Dempsey, J. L. Electrochemical Reduction of Bronsted Acids by Glassy Carbon in Acetonitrile – Implications for Electrocatalytic Hydrogen Evolution. *Inorg. Chem.* **2014**, *53*, 8350-8361.

[31] Nishibayashi, Y. Development of Catalytic Nitrogen Fixation Using Transition Metal–Dinitrogen Complexes under Mild Reaction Conditions. *Dalton Trans.* **2018**, *47*, 11290–11297.

[32] Ashida, Y.; Arashiba, K.; Nakajima, K.; Nishibayashi, Y. Molybdenum-Catalysed Ammonia Production with Samarium Diiodide and Alcohols or Water. *Nature* **2019**, *568*, 536–540.

[33] To crudely estimate the $pK_a$ of $P_3{}^BFe-N_2H$ we assume the upper bound of its $BDFE_{N-H}$ to be ~31 kcal/mol (see 38), the THF gas constant $C_G$ as 59.9 kcal/mol (see ref 36), and the $P_3{}^BFe-N_2{}^{0/-}$ redox couple to be –2.1 V in THF at RT. A lower value for the estimated $BDFE_{N-H}$ of $P_3{}^BFe-N_2H$, for example 28 kcal/mol, instead provides an estimated $pK_a$ of 12 in THF.

[34] Cukier, R. I.; Nocera, D. G. Proton-coupled Electron Transfer. *Annu. Rev. Phys. Chem*. **1998**, *49*, 337-369.

[35] Weinberg, D. E. et al. Proton-coupled Electron Transfer. *Chem. Rev*. **2012**, *7*, 4016-4093.

[36] Agarwal, R. G. et al. Free Energies of Proton-Coupled Electron Transfer Reagents and Their Applications. *Chem. Rev*. **2022**, *122*, 1-49

[37] Tyburski, R.; Liu, T.;  Glover, S. D.; Hammarström, L. Proton-coupled Electron Transfer Guidelines, Fair and Square. *J. Am. Chem. Soc.* **2021**, *143*, 560–576.

[38] Chalkley, M. J.; Peters, J. C. Relating N–H Bond Strengths to the Overpotential for Catalytic Nitrogen Fixation. *Eur. J. Inorg. Chem*. **2020**, 1353-1357.

[39] Chalkley, M. J.; Oyala, P. H.; Peters, J. C. Cp* Noninnocence Leads to a Remarkably Weak C–H Bond via Metallocene Protonation. *J. Am. Chem. Soc.* **2019**, *141*, 4721–4729.

[40] Chalkley, M. J., Garrido-Barros, P. & Peters, J. C. A molecular mediator for reductive concerted Electrocatalytic Reduction of C–C π-Bonds via a Cobaltocene-Derived Concerted Proton–Electron Transfer Mediator: Fumarate Hydrogenation as a Model Study proton-electron transfers via electrocatalysis. *Science,* **2020**, *369*, 850–854.

[41] Derosa, J.; Garrido-Barros, P.; Peters, J. C. Electrocatalytic Reduction of C–C π-Bonds via a Cobaltocene-Derived Concerted Proton–Electron Transfer Mediator: Fumarate Hydrogenation as a Model Study. *J. Am. Chem. Soc.* **2021**, *143*, 9303–9307.

[42] Derosa, J.; Garrido-Barros, P.; Peters, J. C. Electrocatalytic Ketyl-Olefin Cyclization at a Favorable Applied Bias Enabled by a Concerted Proton–Electron Transfer Mediator. *Inorg. Chem.* **2022**, *61*, 6672–6678.

[43] Garrido-Barros, P.; Derosa, J.; Chalkley, M. J.; Peters, J. C. Tandem Electrocatalytic $N_2$ Fixation via Proton-Coupled Electron Transfer. *Nature*, **2022**, 609, 71-76.

[44] Derosa, J.; Garrido-Barros, P.; Li, M.; Peters, J. C. Use of a PCET Mediator Enables Ni-HER Electrocatalyst to Act as a Hydride Delivery Agent. *J. Am. Chem. Soc.* **2022**, *144*, 20118–20125.

[45] Ibrahim, A. F.; Garrido-Barros, P.; Peters, J. C. Electrocatalytic Nitrogen Reduction on a Molybdenum Complex Bearing a PNP Pincer Ligand. *ACS Catalysis*, **2023**, *13*, 72-78.

[46] S. Tshepelevitsh, A. Kütt, M. Lõkov, I. Kaljurand, J. Saame, A. Heering, P. G. Plieger, R. Vianello, I. Leito, On the basicity of organic bases in different media. *Eur. J. Org. Chem*. **2019**, 6735–6748.

[47] Sherbow, T. J.; Thompson, E. J.; Arnold, A.; Sayler, R. I.; Britt, R. D.; Berben, L. A. Electrochemical Reduction of $N_2$ to $NH_3$ at Low Potential by a Molecular Aluminum Complex. *Chem.- Eur. J.* **2019**, *25*, 454–458.

[48] Jeong, E.-Y.; Yoo, C.-Y.; Jung, C. H.; Park, J. H.; Park, Y. C.; Kim, J.-N.; Oh, S.-G.; Woo, Y.; Yoon, H. C. Electrochemical Ammonia Synthesis Mediated by Titanocene Dichloride in Aqueous Electrolytes under Ambient Conditions. *ACS Sustain. Chem. Eng.* **2017**, *5*, 9662–9666.

[49] Saha, P.; Amanullah, S.; Dey, A. Electrocatalytic Reduction of Nitrogen to Hydrazine Using a Trinuclear Nickel Complex. *J. Am. Chem. Soc.*, **2020**, *142*, 17312.

[50] Shipman, M. A.; Symes, M. D. A Re-Evaluation of Sn(II) Phthalocyanine as a Catalyst for the Electrosynthesis of Ammonia. *Electrochim. Acta* **2017**, *258*, 618–622.

[51] Burgess, B. K., Lowe, D. J. Mechanism of Molybdenum Nitrogenase. *Chem. Rev*. **1996**, *96*, 2983-3012.

[52] Einsle, O.; Rees, D. C. Structural Enzymology of Nitrogenase Enzymes. *Chem. Rev*. **2020**, *120*, 4969-5004.

[53] Cowper, N. G. W.; Chernowsky, C. P.; Williams, O. P.; Wickens, Z. K. Potent Reductants via Electron-Primed Photoredox Catalysis: Unlocking Aryl Chlorides for Radical Coupling. *J. Am. Chem. Soc.* **2020**, *142*, 2093–2099.

[54] Kim, H.; Kim, H.; Lambert, T. H.; Lin, S. Reductive Electrophotocatalysis: Merging Electricity and Light To Achieve Extreme Reduction Potentials. *J. Am. Chem. Soc.* **2020**, *142*, 2087–2092.

[55] Miller, D. C.; Tarantino, K. T.; Knowles, R. R. Proton-coupled electron transfer in organic synthesis: fundamentals, applications, and opportunities. *Top. Curr. Chem.* **2016**, *30*, 374–432.

[56] Park, Y.; Kim, S.; Tian, L.; Zhong, H.; Scholes, G. D.; Chirik, P. J. Visible Light Enables Catalytic Formation of Weak Chemical Bonds with Molecular Hydrogen. *Nature Chem.* **2021**, *13*, 969-977.

[57] Johansen, C.; Boyd, E.; Peters, J.C. Catalytic Transfer Hydrogenation of $N_2$ to $NH_3$ via a Photoredox Catalysis Strategy. *Sci. Adv.* **2022**, 8, 43, eade3510.

[58] Ashida, Y. et al. Catalytic Nitrogen Fixation Using Visible Light Energy. *Nature Commun*. **2022**, 13, 7263.